



## Kinetic analysis of DNA compaction by mycobacterial integration host factor at the single-molecule level

Yuanyuan Chen<sup>a,c,d,1</sup>, Zhengyan Zhan<sup>b,1</sup>, Hongtai Zhang<sup>e</sup>, Lijun Bi<sup>e</sup>, Xian-En Zhang<sup>a,c,\*</sup>,  
Yu Vincent Fu<sup>b,f,\*\*</sup>

<sup>a</sup> National Laboratory of Biomacromolecules, CAS Center for Excellence in Biomacromolecules, Institute of Biophysics, Chinese Academy of Sciences, Beijing, 100101, China

<sup>b</sup> State Key Laboratory of Microbial Resources, Institute of Microbiology, Chinese Academy of Sciences, Beijing, 100101, China

<sup>c</sup> University of Chinese Academy of Sciences, Beijing, 100049, China

<sup>d</sup> Core Facility for Protein Research, Institute of Biophysics, Chinese Academy of Sciences, Beijing, 100101, China

<sup>e</sup> Key Laboratory of RNA Biology, Institute of Biophysics, Chinese Academy of Sciences, Beijing, 100101, China

<sup>f</sup> Savaid Medical School, University of Chinese Academy of Sciences, Beijing, 100049, China

### ARTICLE INFO

#### Keywords:

Nucleoid-associated proteins  
Mycobacterial integration host factor (mIHF)  
DNA compaction  
Single-molecule

### ABSTRACT

Nucleoid-associated proteins (NAPs) play an important role on chromosome condensation and organization. Mycobacterial integration host factor (mIHF) is one of the few mycobacterial NAPs identified so far. mIHF has the ability to stimulate mycobacteriophage L5 integration and compact DNA into nucleoid-like or higher order filamentous structures by atomic force microscopy observation. In this study, *M. smegmatis* IHF (MsiHF), which possesses the sequence essential for mIHF's functions, binds 30-bp dsDNA fragments in a sequence-independent manner and displays sensitivity to ion strength in bio-layer interferometry (BLI) experiments. The DNA compaction process of MsiHF was observed at the single-molecule level using the total internal reflection fluorescence microscopy (TIRFM). MsiHF efficiently compacted  $\lambda$  DNA into a highly condensed structure with the concentration of 0.25 and 1.0  $\mu\text{M}$ , and the packing ratios were higher than 10. Further kinetic analysis revealed MsiHF compacts DNA in a three-step mechanism, which consists of two compaction steps with different compacting rates separated by a lag step. This study would help us better understand the mechanisms of chromosomal DNA organization in mycobacteria.

### 1. Introduction

Bacterial chromosomal DNA is compacted in a structure called nucleoid to fit within cells. Meanwhile, DNA must remain accessible for essential processes including DNA replication, transcription, repair, recombination, integration and chromosome segregation [1–3]. Nucleoid organization is controlled by several factors such as nucleoid-associated proteins (NAPs), DNA supercoiling and macromolecular crowding [1]. There are many nucleoid-associated proteins in bacterial cells (such as HU, IHF, H-NS, Fis, Lrp, etc.). These proteins play a central role on chromosome condensation and organization through wrapping, bending, or bridging DNA [1–3].

The variety and functions of NAPs in different Bacteriophyta show obvious diversity. *Mycobacterium tuberculosis* is the pathogen causing

tuberculosis which results in over a million deaths annually. Studies on the basic biological characteristics of *Mycobacterium* will promote the development of new drugs and therapeutic methods. Until now, studies on mycobacteria chromosome organization and NAPs are far fewer than other organisms such as *E. coli*. Compared to other organisms, the type of identified NAPs in mycobacteria is significantly lower, because mycobacterial NAPs share low sequence similarities with those in other bacteria [4]. *Mycobacterium* mainly encodes four types of NAPs, i.e. mHU (HupB), Lsr2 (functional analog of H-NS), EspR and integration host factor (mIHF). *Mycobacterium* species possess an abundant nucleoid-associated protein capable of stimulating the integration of mycobacteriophage L5 DNA, hence designated as integration host factor (mIHF) [5]. BLAST of the protein sequence shows that mIHF homologs are limited in most genera of Actinobacteria, sharing a very low

\* Corresponding author. National Laboratory of Biomacromolecules, CAS center for Excellence in Biomacromolecules, Institute of Biophysics, Chinese Academy of Sciences, Beijing, 100101, China.

\*\* Corresponding author. State Key Laboratory of Microbial Resources, Institute of Microbiology, Chinese Academy of Sciences, Beijing, 100101, China.

E-mail addresses: [zhangxe@ibp.ac.cn](mailto:zhangxe@ibp.ac.cn) (X.-E. Zhang), [fuyu@im.ac.cn](mailto:fuyu@im.ac.cn) (Y.V. Fu).

<sup>1</sup> These authors contributed equally to this work.

sequence similarity with *Escherichia coli* IHF (EciHF). The annotated mIHF in *M. tuberculosis* H37Rv genome (MtIHF) has an N-terminal domain of around 85 amino acids, which is absent from mIHF in *M. smegmatis* (MsIHF) [6,7]. However, some studies have shown that the natural MtIHF is a shorter protein *in vivo* [6], and deletion of the N-terminal 86-amino acid region of MtIHF is dispensable for its functions [8]. These suggest that MsIHF, which is nearly identical to the C-terminal domain of MtIHF, possesses the sequence essential for the known functions of mIHF. Notably, mIHF is essential for the survival of *M. smegmatis* [9] and the growth of *M. tuberculosis* [10], which is in remarkable contrast to its functional analog in *E. coli* (EciHF). In addition, a recent study indicated that mIHF acts as a global regulator to control the genes required for housekeeping functions and pathogenesis in *Mycobacterium tuberculosis* [11].

Some other studies have shown that MtIHF compacts DNA into nucleoid-like or higher order filamentous structures *in vitro* [6,7]. Furthermore, IHF from *Streptomyces coelicolor* (sIHF), a close relative of mIHF, serves important roles on both chromosome condensation and chromosome segregation during *Streptomyces* sporulation [12]. sIHF also affects the activity of topoisomerase both *in vitro* and *in vivo*, consequently altering DNA topology [12]. In a latest study, MsIHF was found to constrain negative DNA supercoils and modulate the activities of prokaryotic topoisomerases in a similar manner [13]. Therefore, these observations imply that mIHF might be involved not only in phage DNA integration but also in chromosomal DNA organization in mycobacteria.

So far, we know very little about the DNA compaction induced by NAPs quantitatively. The DNA compaction by EciHF was studied using force-extension measurements of  $\lambda$  DNA and an analysis of the Brownian motion of small beads tethered to a surface by single short DNA molecules, in equilibrium with an EciHF solution was performed [14]. To investigate the DNA organization by MsIHF, we measured the binding affinity of MsIHF for 30-bp dsDNA fragments using bio-layer interferometry (BLI), and observed the compaction process in real-time at the single-molecule level using the total internal reflection fluorescence microscopy (TIRFM). MsIHF binds 30-bp dsDNA fragments in a sequence-independent manner and the binding is sensitive to ion strength. MsIHF compacts  $\lambda$  DNA efficiently into a highly condensed structure. Kinetic analysis revealed a three-step mechanism of DNA compaction induced by MsIHF, which consists of two compaction steps separated by a lag step.

## 2. Materials and methods

### 2.1. Protein expression and purification

The DNA fragment encoding MsIHF was amplified by PCR using *M. smegmatis* genomic DNA as template. After digestion with NdeI and XhoI, the DNA fragment was cloned into pET28a vector. *E. coli* BL21 cells harboring the plasmid p*Msihf* were grown in Luria-Bertani broth containing 50  $\mu$ g/ml kanamycin at 37 °C to an OD<sub>600</sub> of ~0.6. Overexpression of MsIHF was induced by 0.4 mM isopropyl  $\beta$ -galactopyranoside (IPTG), and the culture was incubated for further 3 h at 37 °C. The recombinant protein was purified by Ni-affinity chromatography (HisTrap column, GE healthcare) and gel filtration chromatography (Superdex 75 column, GE healthcare). The peak fractions of MsIHF in buffer (20 mM Tris-HCl (pH 6.8), 100 mM KCl, 1 mM EDTA) were pooled, concentrated and stored at -80 °C. The MsIHF was identified by peptide mass fingerprint and the protein concentration was determined by BCA method (ThermoFisher).

### 2.2. Kinetic analysis of the interaction of MsIHF with DNA by BLI

BLI experiment was performed at 30 °C on the Octet Red96 system (FortBio). Complementary oligonucleotides N30 (5'-TTTCTACCTTTGGTGCTAATGCCATACT-3') or S30 (5'-TAGAGCCTAGTCTTCCAAA

CTAGCTACGC-3'), including one with a 5'-biotin-label, were immobilized onto streptavidin biosensors about 0.3 nm level. MsIHF proteins were diluted in running buffer (20 mM Tris-Cl, pH 6.8, 100 mM KCl, 1 mM EDTA and 0.05% (v/v) Tween-20), and running buffer containing 50 mM or 150 mM KCl was also performed.

The biosensors were equilibrated in the running buffer for 60 s (baseline), and then incubated with various concentrations (including one buffer well as reference to be subtracted) of MsIHF proteins for 60 s in parallel, followed by 60 s of dissociation in running buffer. The biosensors were regenerated with 1 M NaCl to remove the bound MsIHF. The association rate ( $k_a$ ), dissociation rate ( $k_d$ ) and the equilibrium dissociation constant ( $K_D$ ) were derived using a 1:1 binding model or steady state affinity model (FortBio Data Analysis 8.5 Software).

### 2.3. Single-molecule visualization of DNA compaction by MsIHF

The single-molecule visualization of DNA compaction was carried out as described by Fu et al. previously [15] with some modifications. Flow cell chambers and biotinylated bacteriophage  $\lambda$  DNA were prepared as described previously [16]. The biotinylated  $\lambda$  DNA was then immobilized onto the functionalized surface of the flow cell through the interaction with streptavidin. Free DNA was washed out from the flow cell with blocking buffer (20 mM Tris-Cl, pH6.8, 100 mM KCl, 1 mM EDTA and 0.1 mg/ml BSA). Tethered DNA was stained with SYTOX Orange fluorescent dye (Thermo Fisher Scientific) at a concentration of 10 nM in blocking buffer. To stretch the single-tethered DNA, the flow rates were set at 80  $\mu$ l/min using an aspirating syringe pump (Harvard apparatus, Standard Infuse/Withdraw Pump 11 Elite). MsIHF solution were pumped into the flow cell. A time-lapse movie of the behavior of the immobilized DNA molecules for each experiment was acquired by an inverted Total Internal Reflection Fluorescence microscope (modified from IX-71  $\times$ , Olympus, 60 $\times$  objective with NA = 1.49) with an Andor iXon DU897 EMCCD at 0.1 s exposure and 0.1 s intervals for 800 frames.

DNA length was measured using Matlab 2016a as previously described [15]. For each experiment, the lengths of at least 20 individual DNA molecules were measured. Changes in normalized DNA length of all molecules versus time were plotted and then averaged to export the kinetic curve. The rate of DNA compaction by MsIHF (in  $\mu$ m/s) and the packing ratio of DNA were calculated from each DNA retraction event. The rate of DNA compaction is extracted from the slope of the DNA compacting trajectory. The packing ratio was calculated by the function of the initial length against the final length of DNA. To obtain the compaction rates at variant MsIHF concentrations, each kinetic curve was fit to a multiple-segment line, where the breakpoints were set to be the start- and endpoints of the corresponding steps during DNA compaction. The best linear fit of each compaction step was performed using Origin software with R<sup>2</sup> values > 0.98.

## 3. Results and discussion

Previous studies have shown that MsIHF does not bind preferentially to phage attachment site (*attP*) [5]. Both MtIHF-80 (protein lacking the region of 1–79 amino acids) and sIHF binds DNA in a sequence independent manner [6,12]. However, MtIHF was reported to bind preferentially to the substrate containing *attB* and *attP* sites as well as curved DNA *in vitro* (affinity is 3–5 fold stronger than noncurved DNA) [7]. To better understand the DNA binding properties of MsIHF, we measured the binding affinities of MsIHF for two 30-bp dsDNA fragments (designated N30 and S30, respectively) using BLI assays (Fig. 1). N30 is a non-specific DNA fragment with random sequence, while S30 contains the core sequence in bacterial attachment site (*attB*) which is essential for the integration of phage L5 [17]. The apparent dissociation constants ( $K_D$ ) of MsIHF (in protein dimer) for the two sequences were quite similar (~88 nM for N30 and ~83 nM for S30,

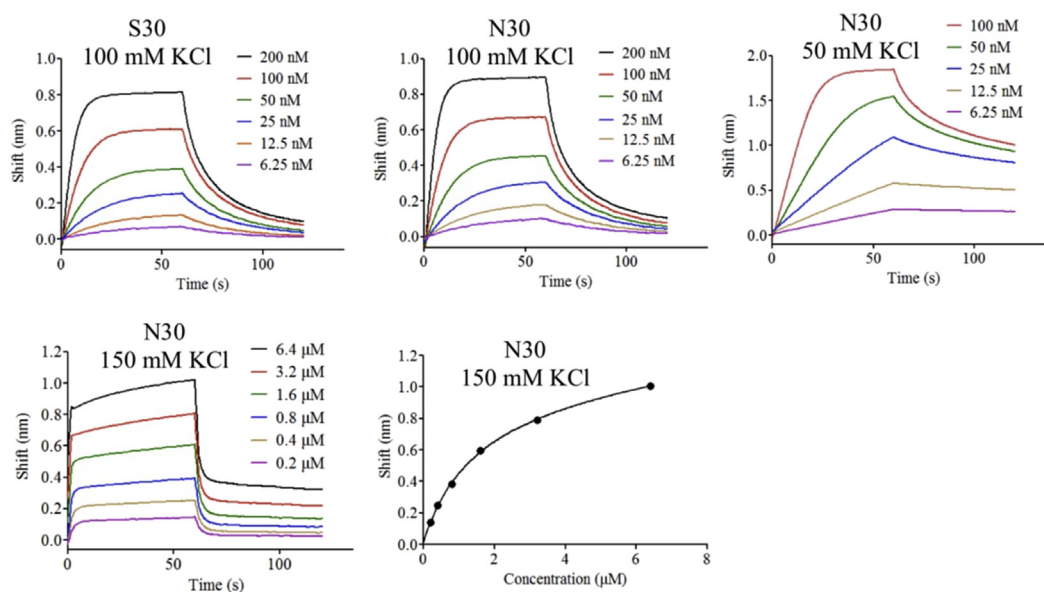


**Fig. 1.** Kinetic characterization of MsiHF binding to DNA by BLI assays. The apparent dissociation constant of MsiHF at 150 mM KCl for N30 was calculated by a fit to steady-state model while others were by a fit to 1:1 binding model.

respectively), suggesting that MsiHF binds to DNA with no sequence preference (Fig. 1). Using EMSA, the  $K_D$  values were found in the range of 0.21–1.5  $\mu\text{M}$  for MtiHF and MtiHF-CTD (a mutant lacking the N-terminal 86 amino acids), binding to the substrates containing *attB* and *attP* sites as well as curved and uncurved DNA [7,8]. The discrepancy between previously reported  $K_D$  [7,8] and the  $K_D$  obtained by BLI in this study is probably due to the differences in the length of DNA substrates (220–600 bp in EMSA vs 30 bp in BLI) and the experimental conditions, e.g. pH 8.0 in EMSA vs pH 6.8 in BLI.

MsiHF bound to N30 DNA with a  $K_D$  value of 15 nM, 88 nM and 2.1  $\mu\text{M}$  in the presence of 50 mM, 100 mM and 150 mM KCl, respectively (Fig. 1), indicating that the binding affinity of MsiHF to short DNA fragments is sensitive to KCl concentration. Sharadamma et al. found that MtiHF forms a salt-stable complex with the DNA fragments containing 600-bp *attB* and 546-bp *attP*, and hypothesized that the salt-stability resulted from the encircling of DNA by the bound MtiHF molecules via protein–protein interactions [7]. Thus, it is likely that mihf might undergo different binding modes on the short and long DNA fragments. Future experiments will be required to address the precise molecular mechanism of two different binding modes.

To investigate the detailed mechanism of DNA compaction induced by MsiHF, we directly observed the length changes of the stretched  $\lambda$  DNA induced by MsiHF at the single-molecule level using TIRFM. Before injecting MsiHF in to the flow cell, the mean end-to-end length of the stretched free  $\lambda$  DNA molecules was  $\sim 13.9 \mu\text{m}$  (Fig. 2A and B, a value nearly 86% of its theoretical length ( $\sim 16.2 \mu\text{m}$ )). After injection of 1  $\mu\text{M}$  of MsiHF protein, the DNA molecules retracted rapidly and finally condensed into a dot with the diameter around 1  $\mu\text{m}$  within 10 s (Fig. 2A). To exclude the possibility that the decrease in DNA length was caused by DNA breaking or other unknown covalently folding, we washed the retracted DNA with blocking solution supplemented with 1 M KCl. After washing with 10-fold volumes of the flow cell, the length of DNA molecule recovered to its initial length of  $\sim 13.6 \mu\text{m}$ , suggesting the DNA compaction was exactly induced by MsiHF in a noncovalent, reversible manner (Fig. 2A and B).

We also measured the kinetics of DNA compaction by MsiHF at four different protein concentrations (1.0, 0.25, 0.10 and 0.04  $\mu\text{M}$ ) to learn more details about the compaction process. Injection of 0.04  $\mu\text{M}$  of MsiHF proteins had no observable effects on the DNA length (Fig. 2C), probably due to that DNA was barely bound by MsiHF proteins at a protein concentration below the  $K_D$  value. In presence of higher protein

concentration, significant DNA retractions were observed (Fig. 2C). The packing ratios at 0.1, 0.25 and 1.0  $\mu\text{M}$  were above 2, 10, and 10 respectively, suggesting the efficient DNA compaction by MsiHF. Notably, the curves showed a three-step mechanism of DNA compaction induced by MsiHF, which actually consists of two compaction steps separated by a lag step (Fig. 2C–F). DNA molecules were all shortened by about 20% in the first compacting step. The compaction rates in this step ( $v_1$ ) were 0.23, 1.59 and 3.14  $\mu\text{m/s}$  at MsiHF concentrations of 0.1, 0.25 and 1.0  $\mu\text{M}$ , respectively (Fig. 2D–F). In the lag step, the length of DNA molecules remained largely unchanged. The duration of this step dropped significantly with the increment of protein concentration ( $\sim 43.1$  s at 0.1  $\mu\text{M}$ ,  $\sim 15.6$  s at 0.25  $\mu\text{M}$ , and  $\sim 2.4$  s at 1.0  $\mu\text{M}$ , respectively) (Fig. 2D–F). After the lag step, DNA molecules continued to retract in the second compaction step and finally condensed into a dot at protein concentrations of 0.25 and 1.0  $\mu\text{M}$  (Fig. 2E and F). In presence of 0.1  $\mu\text{M}$  of MsiHF, DNA length also dropped steadily in this step although the complete condensation was not observed within the observation time (100 s) (Fig. 2D). The compaction rates ( $v_2$ ) in this step are 0.10, 0.47 and 1.98  $\mu\text{m/s}$  at MsiHF concentrations of 0.1, 0.25 and 1.0  $\mu\text{M}$ , respectively (Fig. 2D–F). The multistep pattern of MsiHF induced DNA compaction implies that MsiHF might serve multiple architectural roles in chromosomal DNA organization. First, MsiHF might act as a DNA bender since the C-terminal domain of MtiHF (mihf-80) is capable of introducing bends with variable degree in plasmid DNA [6]. Given the bending angle in linear DNA introduced by mihf-80 appeared to be in the range of  $60^\circ$  to  $80^\circ$  [6], the end-to-end length of the bent DNA would be estimated to be 11–17% shorter than that of the unbound DNA, which is in consent with our observations of the  $\sim 20\%$  DNA retraction in the first compaction step. Second, after bending DNA, MsiHF might compact DNA into a higher order structures through protein-protein and/or protein-DNA interactions. For instance, binding of MtiHF could induce encircling of DNA via protein-protein interactions and the formation of a salt-stable complex [7]. Crystal structure of the sIHf-DNA complex revealed two distinct DNA-contacting regions on the protein surface [12], which are also conserved in MsiHF. Accordingly, the bound MsiHF dimers may interact with the adjacent DNA regions to form higher-order structures after the DNA molecule is saturated by MsiHF proteins. The changes in DNA geometry induced by bound MsiHF might also contribute to this process [13], as DNA supercoiling facilitates high-order DNA organization [3]. Therefore, the lag step between the two compaction steps could reflect the

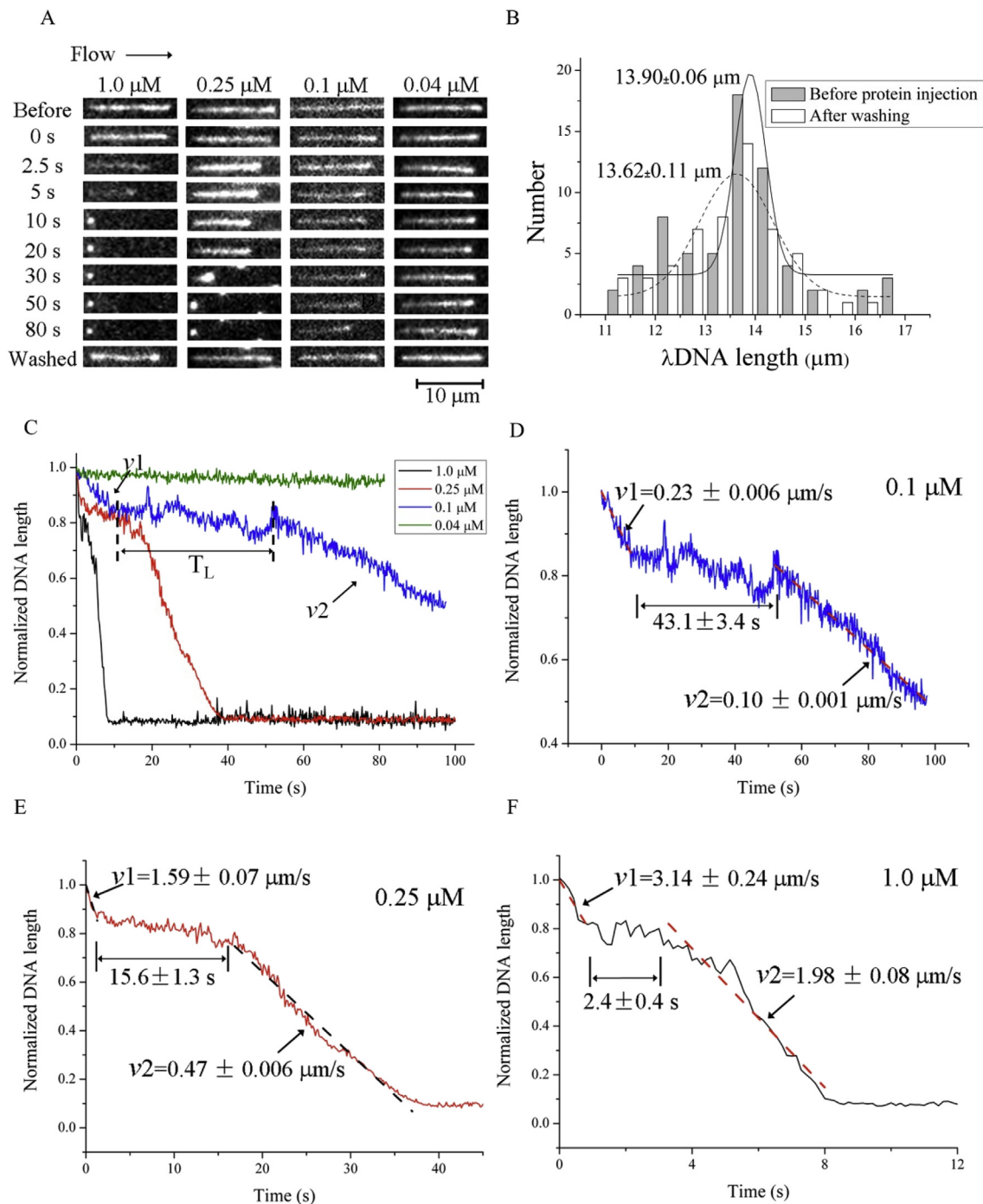


**Fig. 2.** DNA compaction process of MsiHF at the single-molecule level. (A) Single-molecule visualization of  $\lambda$  DNA compaction induced by MsiHF. Frames at the indicated time points of a representative single DNA molecule from the video recorded at each protein concentration are plotted as a montage. (B) Histograms of the end-to-end length of DNA molecules before protein injection and after washing. The mean lengths were calculated by Gaussian fit. (C) Averaged kinetic curves for DNA compaction at different MsiHF concentrations. The interval between the two DNA compaction steps (separated by dashed lines) is labeled on the curve for 0.1  $\mu\text{M}$  of MsiHF as an example.  $v_1$ , compaction rate of the first step;  $T_L$ , duration of the second step; and,  $v_2$ , compaction rate of the third step. (D–F) Zoom-in views of the curves in (C) with the linear fit for each compaction step in the DNA retraction trajectories shown in dashed line. The corresponding compaction rate for each step was calculated by using a mean initial DNA length of 13.9  $\mu\text{m}$ .

rearrangement of MsiHF proteins on DNA.

In this study, we show that MsiHF binds DNA with no sequence preference and compacts DNA efficiently. The single-molecule assay revealed a three-step mechanism of the MsiHF induced DNA compaction, which is initiated by DNA bending, followed by rearrangement of MsiHF on DNA and further assemble into nucleoid-like structures. These results agree well with the findings that MtiHF promotes DNA compaction into nucleoid-like or higher order filamentous structures

[7]. Notably, our results enable better understanding the mechanisms of chromosomal DNA organization in mycobacteria, which might have potential significance for development of drugs targeting miHF.

#### Conflicts of interest

The authors declare no conflict of interest.

## Acknowledgments

We thank Zhenwei Yang, Bingxue Zhou at Core Facility for Protein Research (Institute of Biophysics, CAS) for technical help with BLI experiments. This work was funded by the Strategic Priority Research Program of the Chinese Academy of Sciences (Grant No. XDB29050101 to X.E. Zhang), and from the National Natural Science Foundation of China (31401059 to ZY. Zhan, 31371264 to Y. V. Fu and 31770150 to L.J. Bi).

## References

- [1] Dame RT. The role of nucleoid-associated proteins in the organization and compaction of bacterial chromatin. *Mol Microbiol* 2005;56:858–70.
- [2] Dillon SC, Dorman CJ. Bacterial nucleoid-associated proteins, nucleoid structure and gene expression. *Nat Rev Microbiol* 2010;8:185–95.
- [3] Badrinarayanan A, Le TB, Laub MT. Bacterial chromosome organization and segregation. *Annu Rev Cell Dev Biol* 2015;31:171–99.
- [4] Kriel NL, Gallant J, van Wyk N, van Helden P, Sampson SL, Warren RM, Williams MJ. Mycobacterial nucleoid associated proteins: an added dimension in gene regulation. *Tuberculosis* 2018;108:169–77.
- [5] Pedulla ML, Lee MH, Lever DC, Hatfull GF. A novel host factor for integration of mycobacteriophage L5. *Proc Natl Acad Sci USA* 1996;93:15411–6.
- [6] Mishra A, Vij M, Kumar D, Taneja V, Mondal AK, Bothra A, Rao V, Ganguli M, Taneja B. Integration host factor of Mycobacterium tuberculosis, mlHF, compacts DNA by a bending mechanism. *PLoS One* 2013;8:e69985.
- [7] Sharadamma N, Harshavardhana Y, Ravishankar A, Anand P, Chandra N, Muniyappa K. Molecular dissection of Mycobacterium tuberculosis integration host factor reveals novel insights into the mode of DNA binding and nucleoid compaction. *Biochemistry* 2015;54:4142–60.
- [8] Sharadamma N, Harshavardhana Y, Muniyappa K. Defining the functionally important domain and amino acid residues in Mycobacterium tuberculosis integration host factor for genome stability, DNA binding, and integrative recombination. *J Bacteriol* 2017;199.
- [9] Pedulla ML, Hatfull GF. Characterization of the mlHF gene of Mycobacterium smegmatis. *J Bacteriol* 1998;180:5473–7.
- [10] Sasseti CM, Boyd DH, Rubin EJ. Genes required for mycobacterial growth defined by high density mutagenesis. *Mol Microbiol* 2003;48:77–84.
- [11] Odermatt NT, Sala C, Benjak A, Cole ST. Essential nucleoid associated protein mlHF (Rv1388) controls virulence and housekeeping genes in Mycobacterium tuberculosis. *Sci Rep* 2018;8:14214.
- [12] Swiercz JP, Nanji T, Gloyd M, Guarne A, Elliot MA. A novel nucleoid-associated protein specific to the actinobacteria. *Nucleic Acids Res* 2013;41:4171–84.
- [13] Chen YY, Zhang XE, Bi LJ. Effects of integration host factor (IHF) from Mycobacterium smegmatis on DNA topological structure. *Prog Biochem Biophys* 2017;44:1110–7.
- [14] Ali BM, Amit R, Braslavsky I, Oppenheim AB, Gileadi O, Stavans J. Compaction of single DNA molecules induced by binding of integration host factor (IHF). *Proc Natl Acad Sci U S A* 2001;98:10658–63.
- [15] Chen XQ, Zhao ES, Fu YV. Using single-molecule approach to visualize the nucleosome assembly in yeast nucleoplasmic extracts. *Sci Bull* 2017;62:399–404.
- [16] Yardimci H, Loveland AB, van Oijen AM, Walter JC. Single-molecule analysis of DNA replication in Xenopus egg extracts. *Methods* 2012;57:179–86.
- [17] Pena CEA, Stoner JE, Hatfull GF. Positions of strand exchange in mycobacteriophage L5 integration and characterization of the attB site. *J Bacteriol* 1996;178:5533–6.